Thermal Conductivity of Group VA Puckered Monolayer Structures

Tuğbey Kocabaş[1], Deniz Çakır[2], Oğuz Gülseren[3], Feridun Ay[4], Nihan Kosku Perkgöz[4], Cem Sevik[5]

[1]Department of Advanced Technologies, Graduate School of Sciences, Anadolu University, Eskisehir, TR 26555, Turkey, [2]Department of Physics and Astrophysics, University of North Dakota, Grand Forks, North Dakota 58202, USA, [3]Department of Physics, Bilkent University, Bilkent, Ankara 06800, Turkey, [4]Department of Electrical and Electronics Engineering, Faculty of Engineering, Anadolu University, Eskisehir, TR 26555, Turkey, [5]Department of Mechanical Engineering, Faculty of Engineering, Anadolu University, Eskisehir, TR 26555, Turkey

1. Structure

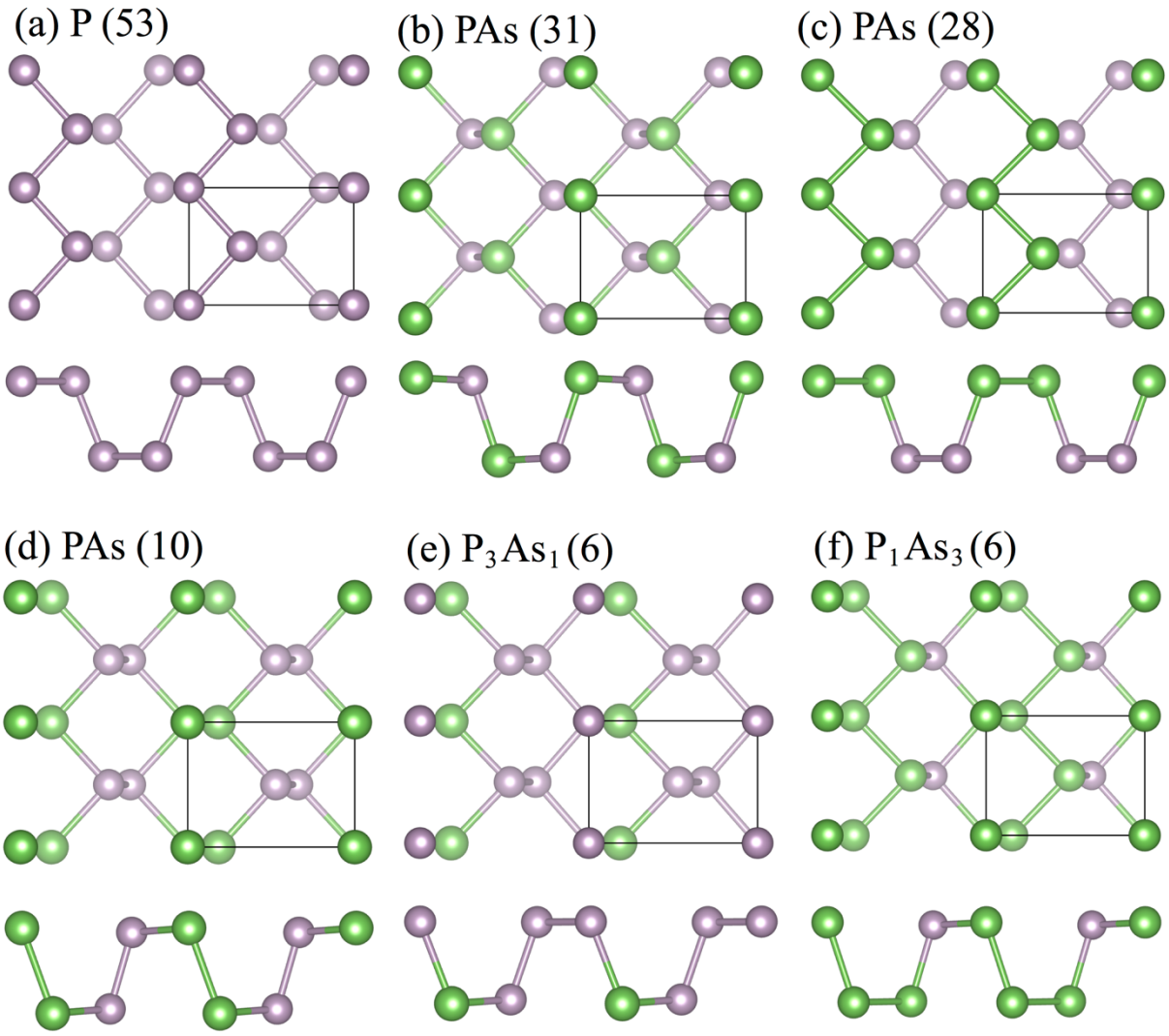

Figure 1: Schematical representation of Group VI compound semiconductors. (a) Represents pristine P, As, Sb and Bi structures, (b) represents $X_{0.5}Y_{0.5}$, (X = P, As, Sb, Bi, Y = P, As, Sb, Bi, and X ≠ Y) structures with space group symmetry 31, (c) represents $X_{0.5}Y_{0.5}$, (X = P, As, Sb, Bi, Y = P, As, Sb, Bi, and X ≠ Y) structures with space group symmetry 28, (d) represents $X_{0.5}Y_{0.5}$, (X = P, As, Sb, Bi, Y = P, As, Sb, Bi, and X ≠ Y) structures with space group symmetry 10, and (e, f) represents $X_{0.25}Y_{0.75}$, (X = P, As, Sb, Bi, Y = P, As, Sb, Bi, and X ≠ Y) structures with space group symmetry 6.

2. Phonon Dispersions

a. Pristine Structure

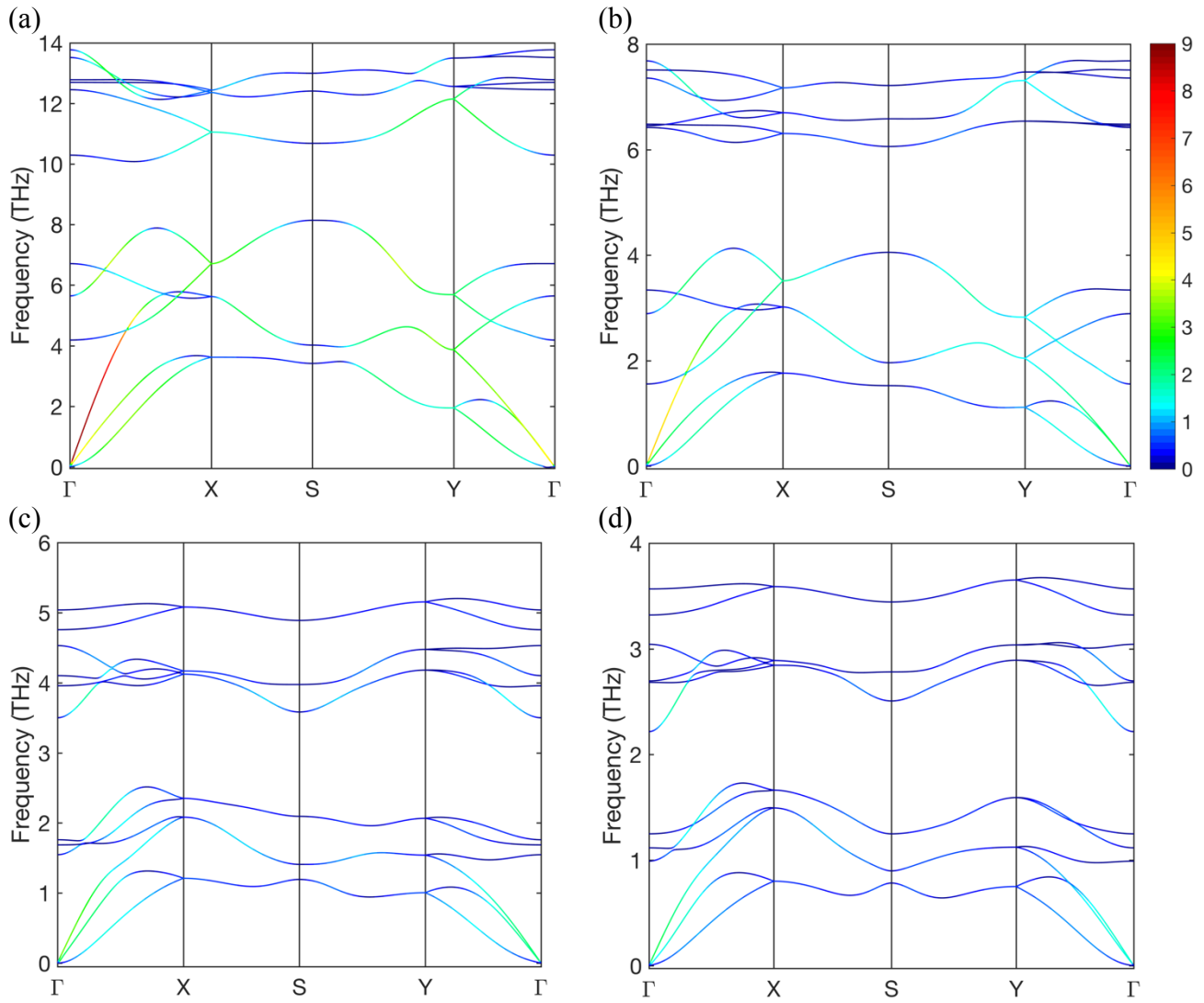

Figure 2: Phonon dispersion curves together with group velocities in km/s (depicted as line color) along the high-symmetry directions of the first Brillouin zone. (a) P, (b) As, (c) Sb, and (d) Bi.

b. X_2Y_2, (X = P, As, Sb, Bi, Y = P, As, Sb, Bi, and X ≠ Y) Compound Structures

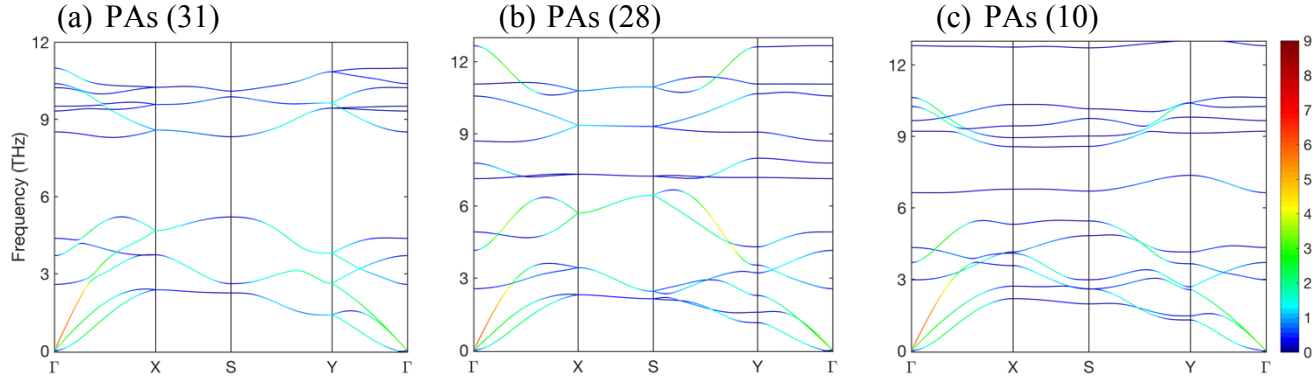

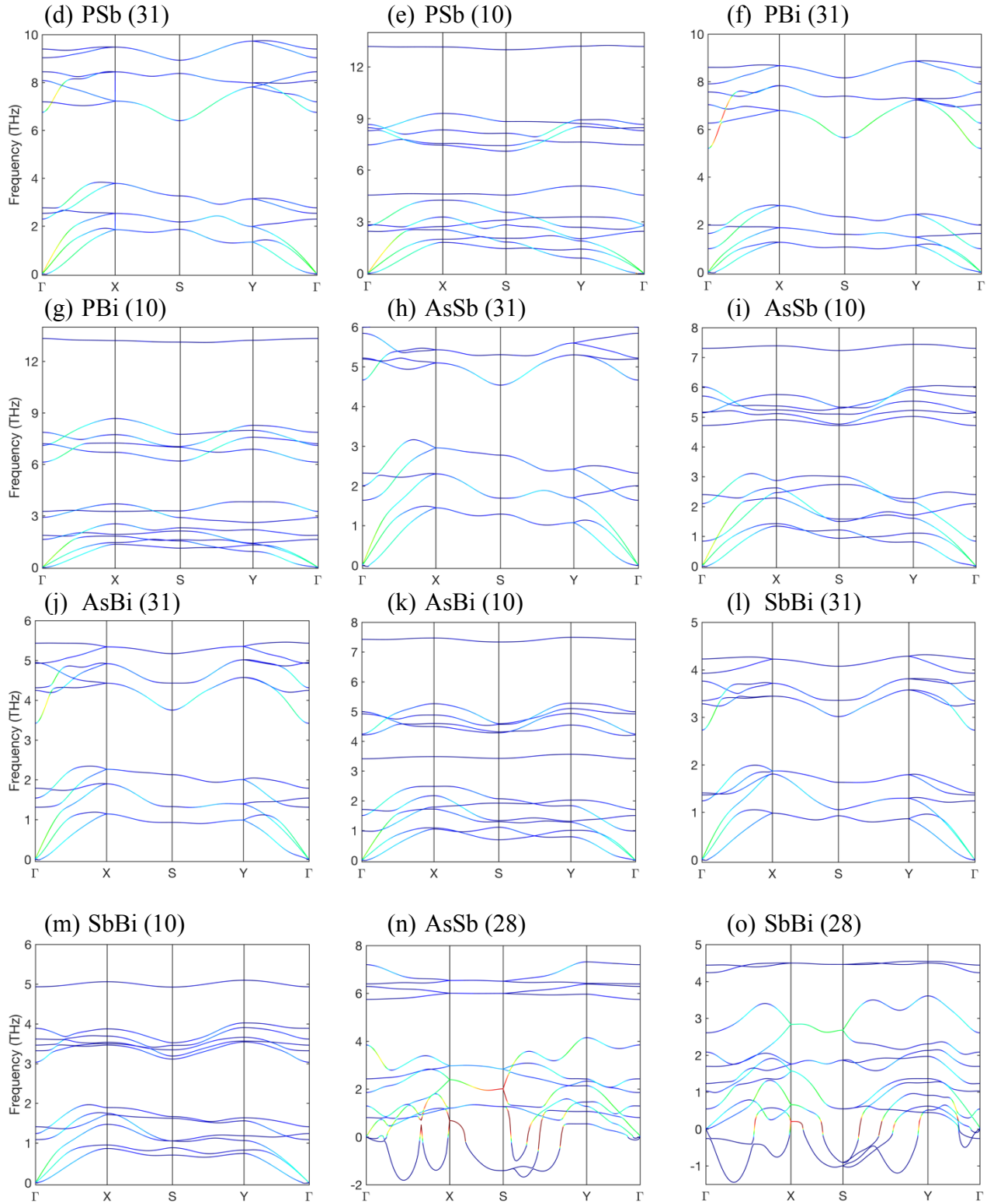

Figure 3: Phonon dispersion curves together with group velocities in km/s (depicted as line color) along the high-symmetry directions of the first Brillouin zone. (n) and (o) are depicted as examples of unstable structures.

c. X_1Y_3, (X = P, As, Sb Y = P, As, Sb and X ≠ Y) Compound Structures

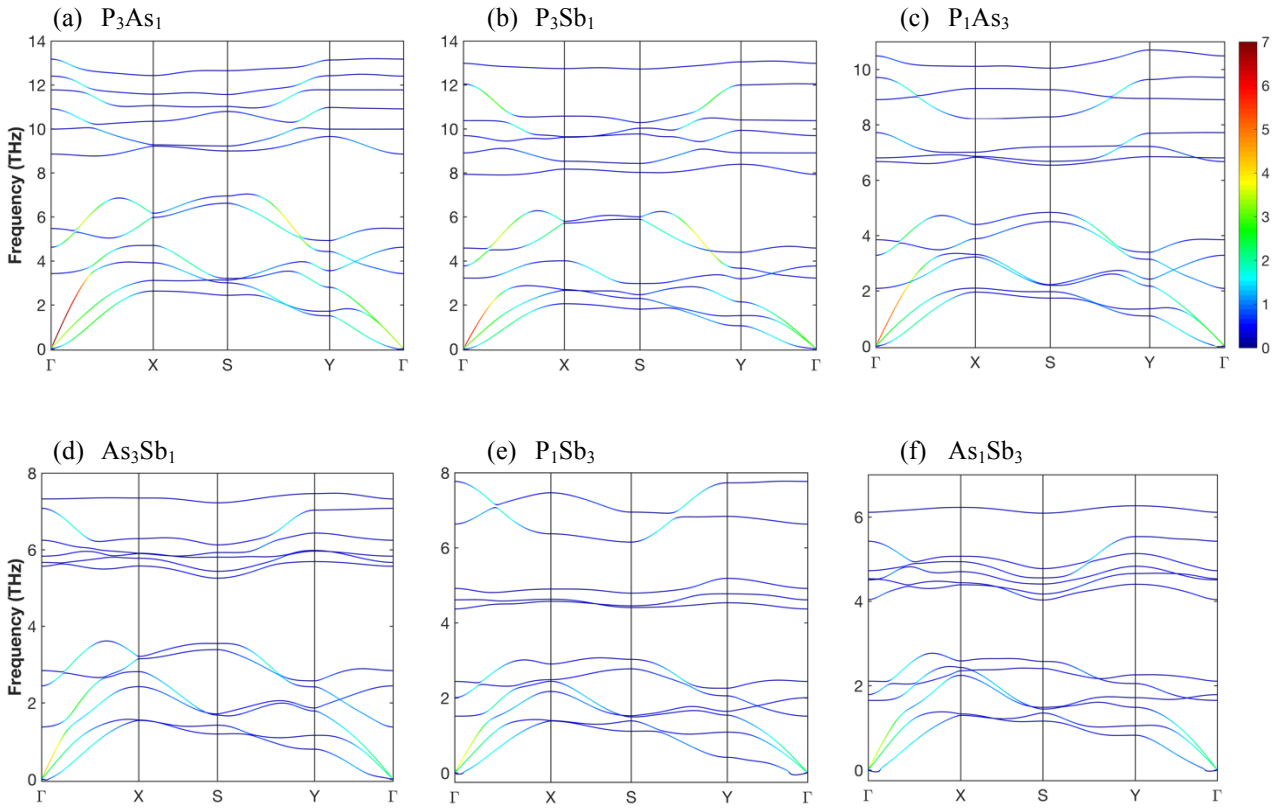

Figure 4: Phonon dispersion curves together with group velocities in km/s (depicted as line color) along the high-symmetry directions of the first Brillouin zone.

3. Debye Temperature

TABLE I: The calculated average effective masses of the structures, Debye temperature, and δ.

	Space Group	*Mass* (au)	θ_D (K)	δ (Å)
P	53	30.9730	206	1.9530
P_3As_1	6	41.4602	165	1.9926
PAs	31	51.9473	134	2.0271
PAs	28	51.9473	130	2.0400
PAs	10	51.9473	147	2.0229
P_3Sb_1	6	53.6698	132	2.0491
P_1As_3	6	62.4345	118	2.0649
As	53	72.9216	101	2.0951
PSb	31	76.3665	103	2.0791
PSb	10	76.3665	98	2.1008
As_3Sb_1	6	85.1312	88	2.1431
AsSb	31	97.3408	83	2.1599
AsSb	10	97.3408	80	2.1877
PBi	31	119.9765	70	2.1406
PBi	10	119.9765	73	2.1284
Sb	31	121.7600	74	2.2727
AsBi	31	140.9508	65	2.2074
AsBi	10	140.9508	61	2.2153
SbBi	31	165.3700	56	2.3124
SbBi	10	165.3700	51	2.3513
Bi	31	208.9800	50	2.3533

4. Graphene

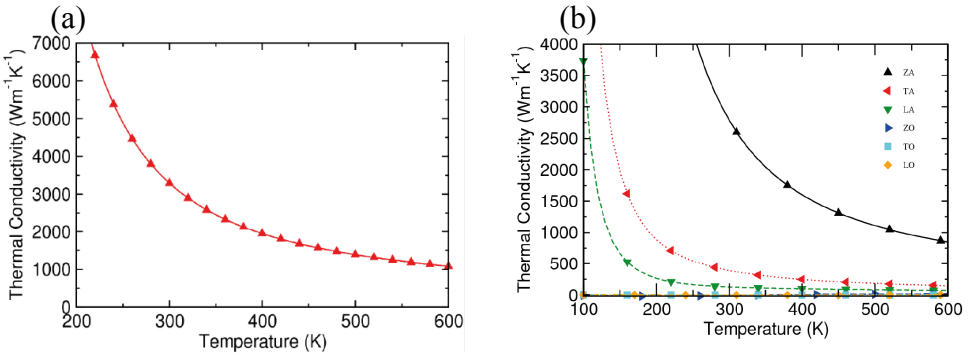

Figure 5: (a) The calculated Thermal Conductivity for Graphene. (b) Calculated thermal conductivity of individual modes. This data is obtained by using the following computational parameters: PBE Pseudopotential, 500 eV energy cut-off, and 6x6x1 k-point grid for all the simulations, 6x6x1 super cell structure for the 2nd and 3rd order force constant calculations, maximum 9 nearest neighbour interactions for the 3rd order force constant calculations, and 100x100x1 q-point grid for the thermal conductivity calculations.

5. Room Temperature Thermal conductivity

a. Pristine Structures

TABLE II: The calculated room temperature κ of the structures, together with the results reported in the literature. The values reported by Zheng *et. al.* are modified by the out of plane distance used in our study. G. Zheng, Y. Jia, S. Gao, and S.-H. Ke, Phys. Rev. B 94, 155448 (2016).

Structure	Zigzag		Armchair	
	This Work	Zheng *et al.*	This Work	Zheng *et al.*
P	109.6	109.9	21.0	23.5
As	20.0	26.8	5.6	5.7
Sb	9.5	9.7	5.3	4.7
Bi	4.1		2.0	

b. Binary Compounds: XY, (X = P, As, Sb, Bi, Y = P, As, Sb, Bi, and X ≠ Y) structures

TABLE III: The calculated room temperature κ of the 50% compound structures.

Structure	Space Group	Zigzag	Armchair
PAs	31	38.6	8.4
PAs	28	45.7	7.9
PAs	10	41.2	5.9
PSb	31	26.1	14.3
PSb	28	UNSTABLE	
PSb	10	13.1	3.1
PBi	31	5.7	4.9
PBi	28	UNSTABLE	
PBi	10	6.0	1.5
AsSb	31	9.5	4.4
AsSb	28	UNSTABLE	
AsSb	10	8.9	2.1
AsBi	31	8.0	4.3
AsBi	28	UNSTABLE	

AsBi	10	8.8	3.8
SbBi	31	6.1	2.5
SbBi	28	UNSTABLE	
SbBi	10	7.3	3.6

c. One-Third Compounds: XY, (X = P, As, Sb, Bi, Y = P, As, Sb, Bi, and X ≠ Y) structures

TABLE IV: The calculated room temperature κ of the 25% compound structures.

Structure	Space Group	Zigzag	Armchair
P_3As_1	6	64.1	11.4
P_3Sb_1	6	31.4	3.5
P_1As_3	6	25.5	4.6
As_3Sb_1	6	11.0	2.4

6. Electronic Structure

a. Pristine Structures

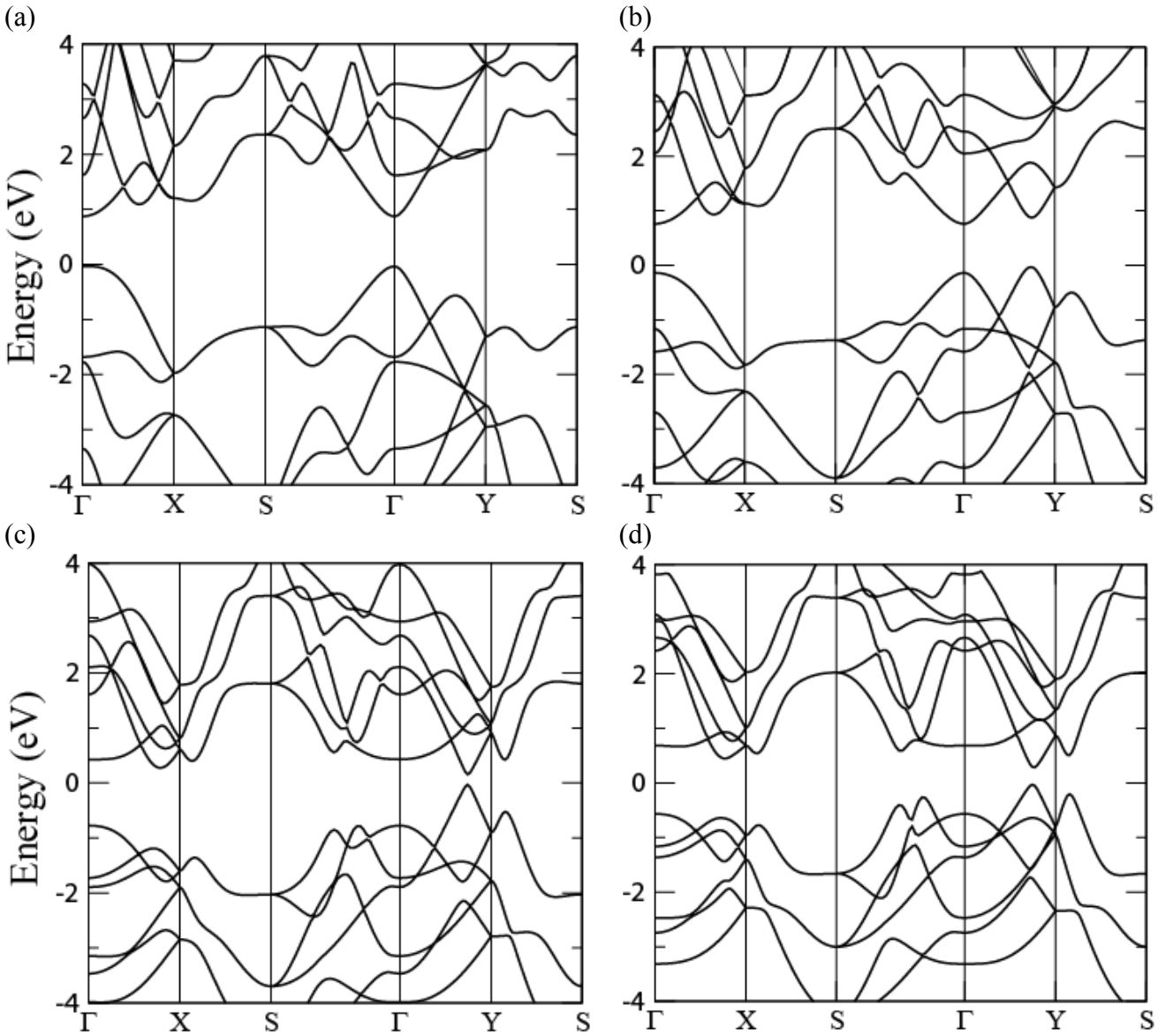

Figure 6: Electronic band structure along the high-symmetry directions of the first Brillouin zone. (a) P, (b) As, (c) Sb, and (d) Bi.

b. X_2Y_2, (X = P, As, Sb, Bi, Y = P, As, Sb, Bi, and X ≠ Y) Compound Structures

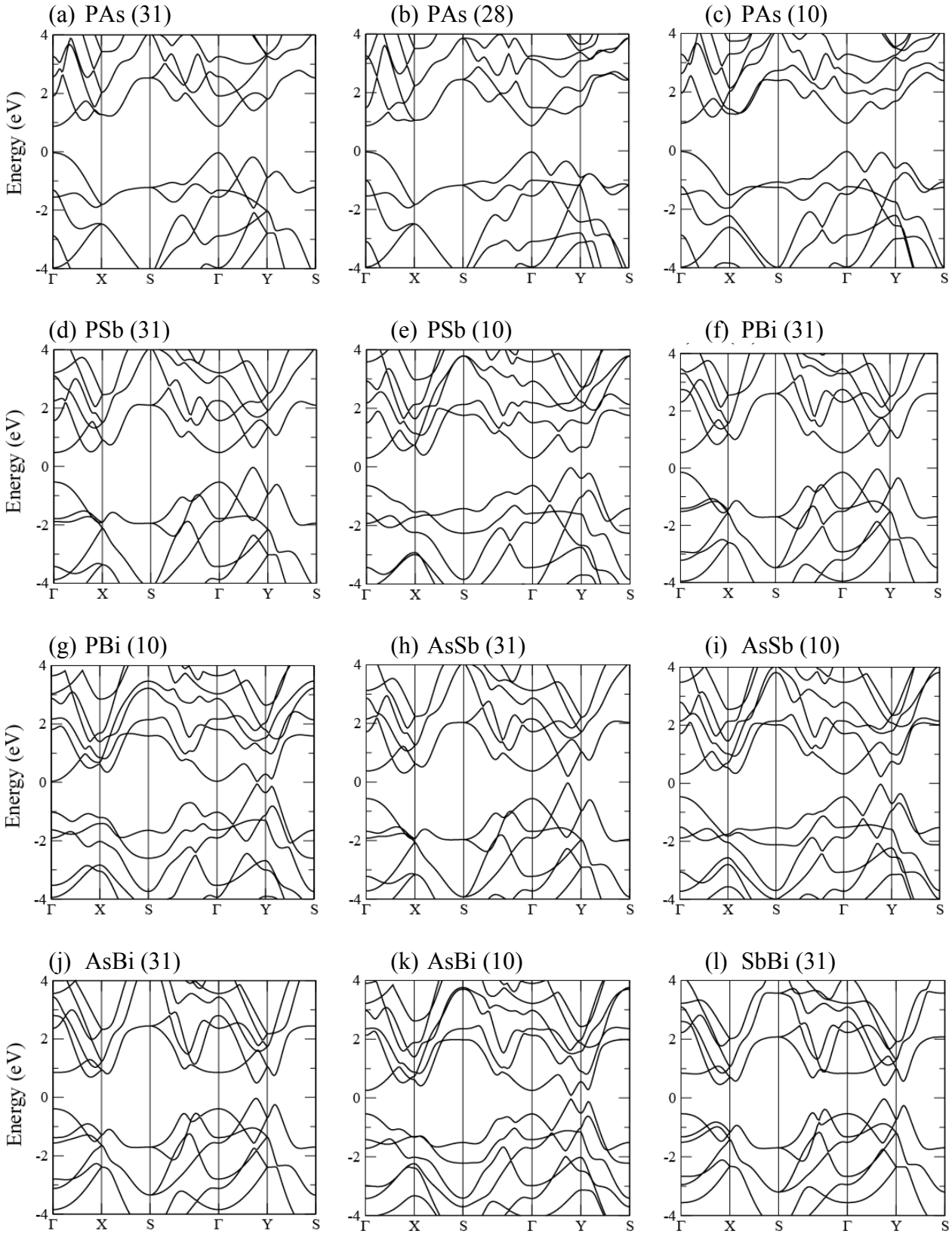

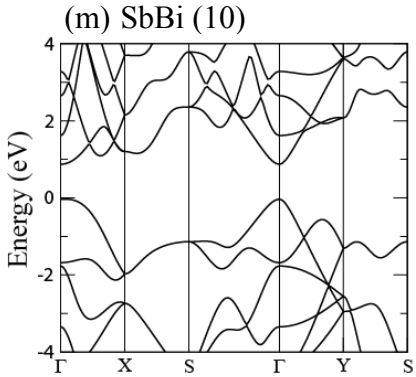

Figure 7: Electronic band structure of 50% compounds along the high-symmetry directions of the first Brillouin zone.

c. X_1Y_3, (X = P, As, Sb Y = P, As, Sb and X ≠ Y) Compound Structures

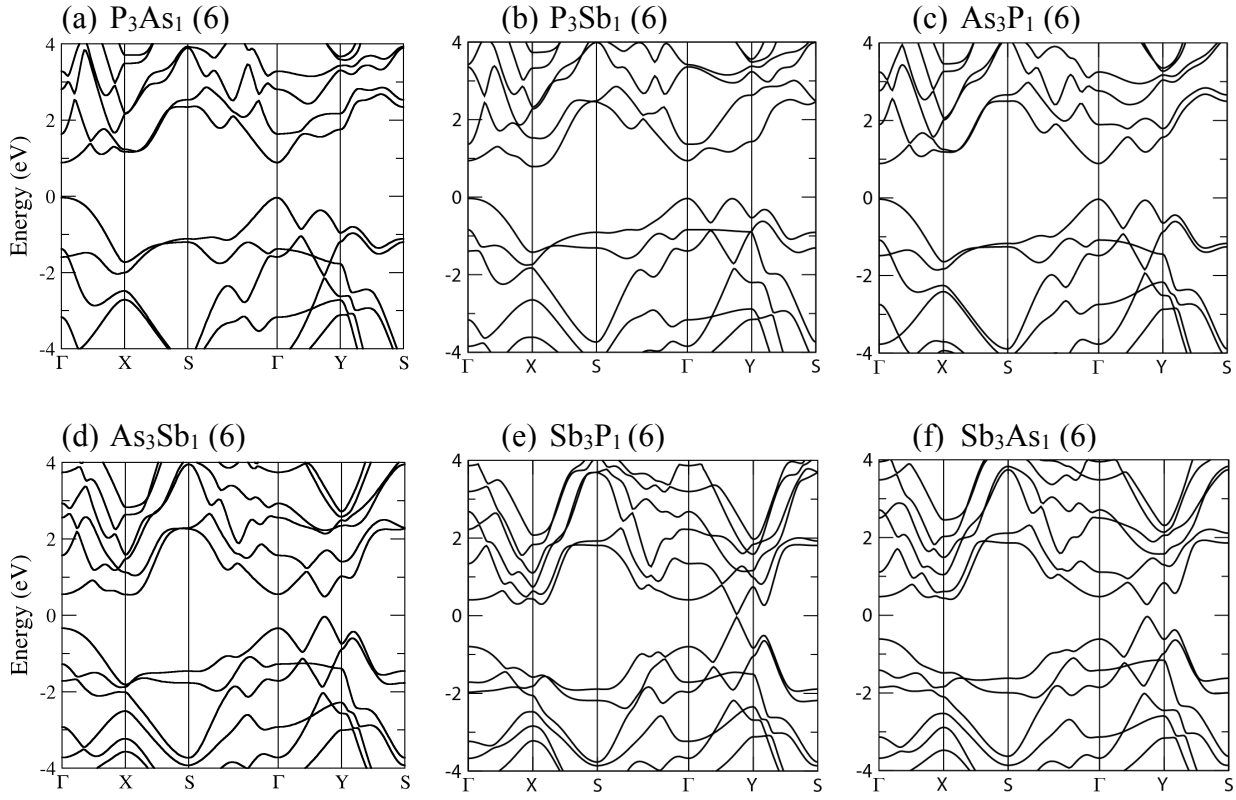

Figure 8: Electronic band structure of 25% compounds along the high-symmetry directions of the first Brillouin zone.

7. Structural Properties

TABLE V: The calculated lattice constants, a_0 and b_0, structural angles, A_1, A_2, and A_3, electronic band gap, E_{GAP} (Indirect gaps are depicted as bold face), and Cohesive Energy.

	Space Group	a_0 (Å)	b_0 (Å)	A_1 (Θ)	A_2 (Θ)	A_3 (Θ)	E_{GAP} (eV)	Cohesive Energy * (eV/Atom)
P	38	3.29	4.62	104.16	104.16	95.92	0.91 Γ➡Γ	-3.447
As	38	3.68	4.76	100.64	100.64	94.5	**0.79 Γ-Y➡Γ**	-2.926
Sb	38	4.35	4.74	102.56	88.61	95.33	0.19 Γ-Y➡Γ-Y	-2.613
Bi	38	4.56	4.84	103.74	85.23	93.97	0.31 Γ-Y➡Γ-Y	-2.718
PAs	31	3.50	4.69	100.22	104.09	94.92	0.90 Γ➡Γ	-3.153
PAs	28	3.46	4.81	103.72	102.49	99.39	0.89 Γ➡Γ	-3.155
PAs	10	3.50	4.68	100.42	100.42	94.84	0.96 Γ➡Γ	-3.173
P_3As_1	6	3.39	4.68	103.28	101.64	92.47	0.92 Γ➡Γ	-3.307
P_1As_3	6	3.58	4.76	100.03	101.65	92.35	0.92 Γ➡Γ	-3.034
PSb	31	3.90	4.42	104.94	89.91	96.43	**0.51 Γ-Y➡Γ**	-2.967
PSb	10	3.85	4.58	93.75	93.76	95.15	**0.34 Γ-Y➡Γ**	-2.990
P_3Sb_1	6	3.54	4.47	102.48	96.94	88.29	**0.82 Γ➡X**	-3.166
P_1Sb_3	6	4.07	4.85	103.98	96.68	100.14	0.31 Γ-Y➡Γ-Y	-2.750
PBi	31	4.10	4.69	100.87	91.42	96.77	**0.58 Γ-Y➡Γ**	-2.846
PBi	10	4.03	4.48	101.87	101.87	95.24	0.09 Γ-Y➡Γ-Y	-2.889
AsSb	31	4.05	4.60	103.14	90.97	95.78	0.24 Γ-Y➡Γ-Y	-2.774
AsSb	10	4.02	4.75	95.71	95.72	95.14	0.28 Γ-Y➡Γ-Y	-2.767
As_3Sb_1	6	3.85	4.77	100.6	95.47	91.61	0.52 Γ-Y➡Γ-Y	-2.834
As_1Sb_3	6	4.20	4.73	100.17	89.76	92.30	0.07 Γ-Y➡Γ-Y	-2.679
AsBi	31	4.23	4.60	91.65	99.68	96.13	0.53 Γ-Y➡Γ-Y	-2.686
AsBi	10	4.19	4.67	99.57	99.57	95.49	0.13 Γ-Y➡Γ-Y	-2.679
SbBi	31	4.47	4.78	102.56	87.08	94.74	0.46 Γ-Y➡Γ-Y	-2.531
SbBi	10	4.48	4.93	96.06	93.34	95.35	0.27 Γ-Y➡Γ-Y	-2.530

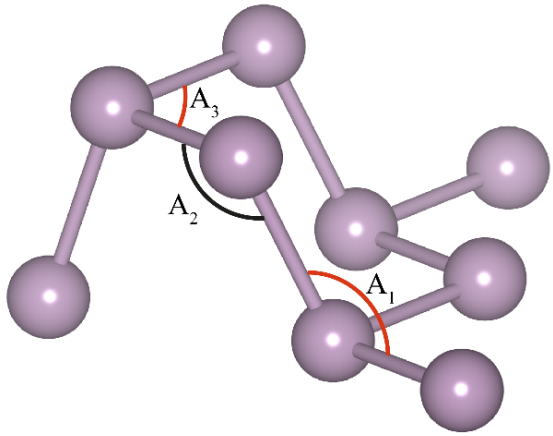

* The cohesive energies are calculated by subtracting the individual atom energies from total energy of the system.

8. Mean Free Paths

a. Pristine Structures

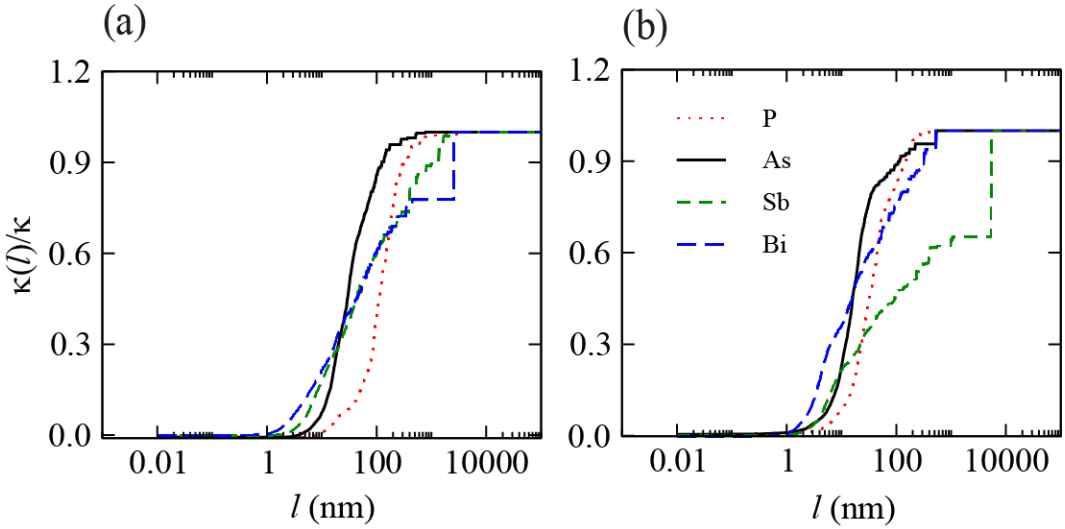

Figure 9: Calculated cumulative thermal conductivity of pristine structures as a function of mean free path at T=300K along the (a) zigzag and (b) armchair directions

b. X_2Y_2, (X = P, As, Sb, Bi, Y = P, As, Sb, Bi, and X ≠ Y) Compound Structures

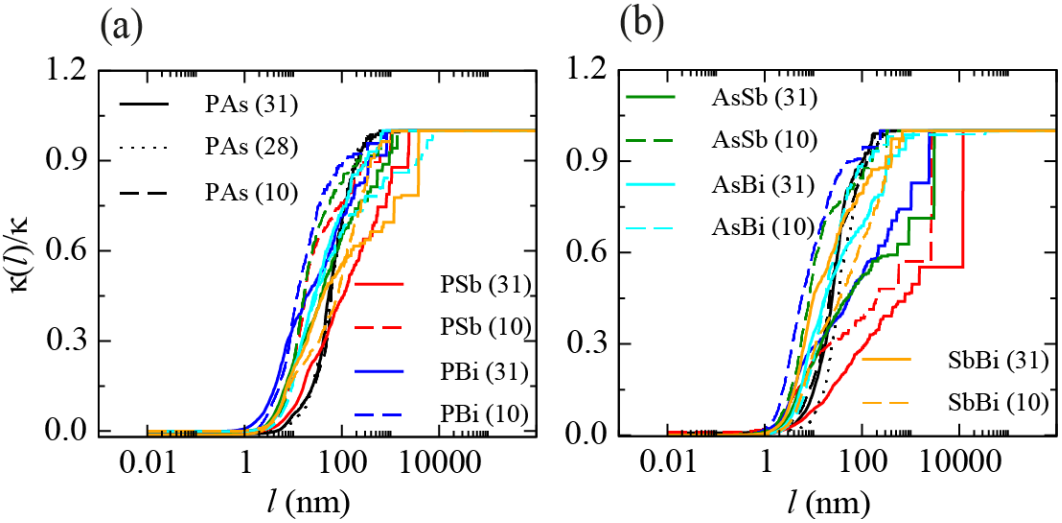

Figure 10: Calculated cumulative thermal conductivity of 50% compound structures as a function of mean free path at T=300K along the (a) zigzag and (b) armchair directions

c. X_1Y_3, (X = P, As, Sb Y = P, As, Sb and X ≠ Y) Compound Structures

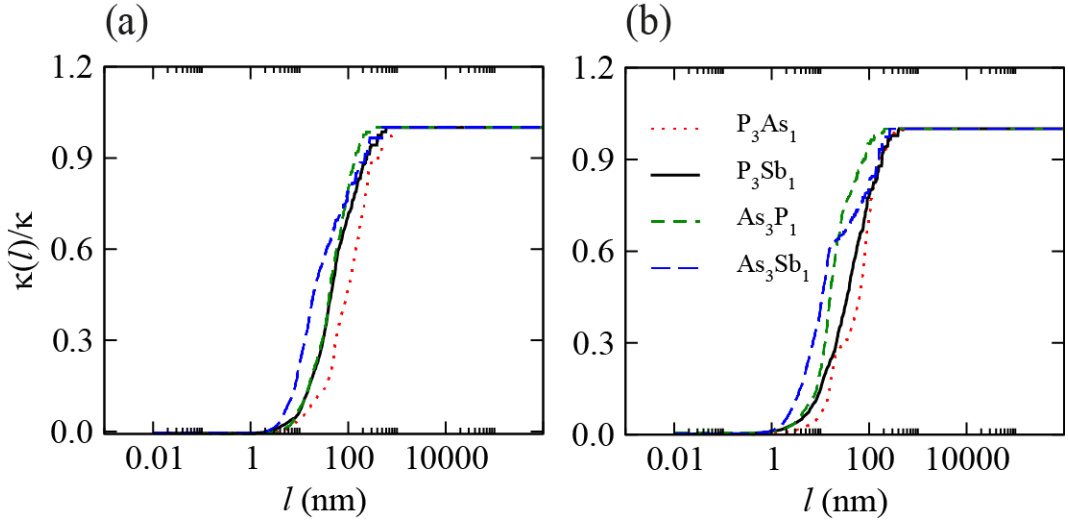

Figure 11: Calculated cumulative thermal conductivity of 25% compound structures as a function of mean free path at T=300K along the (a) zigzag and (b) armchair directions

9. Iterative Method versus RTA

a. Pristine Structures

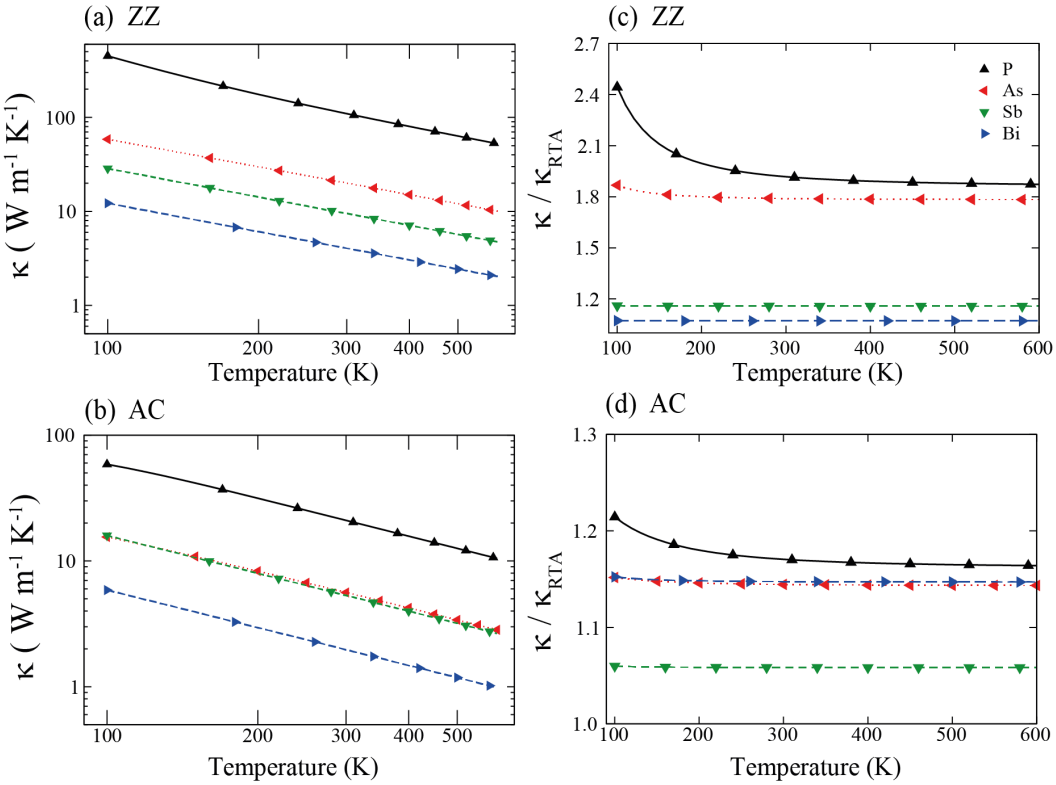

Figure 9: Thermal conductivity of pristine structures as a function of temperature along the (a) zigzag and (b) armchair direction calculated by the self-consistent solution of Peierls-BTE and ratio of the self consistent (κ) and zeroth order (corresponding to the κ_{RTA}) solutions are also depicted for (c) zigzag and (d) armchair directions.

b. X_2Y_2, (X = P, As, Sb, Bi, Y = P, As, Sb, Bi, and X ≠ Y) Compound Structures

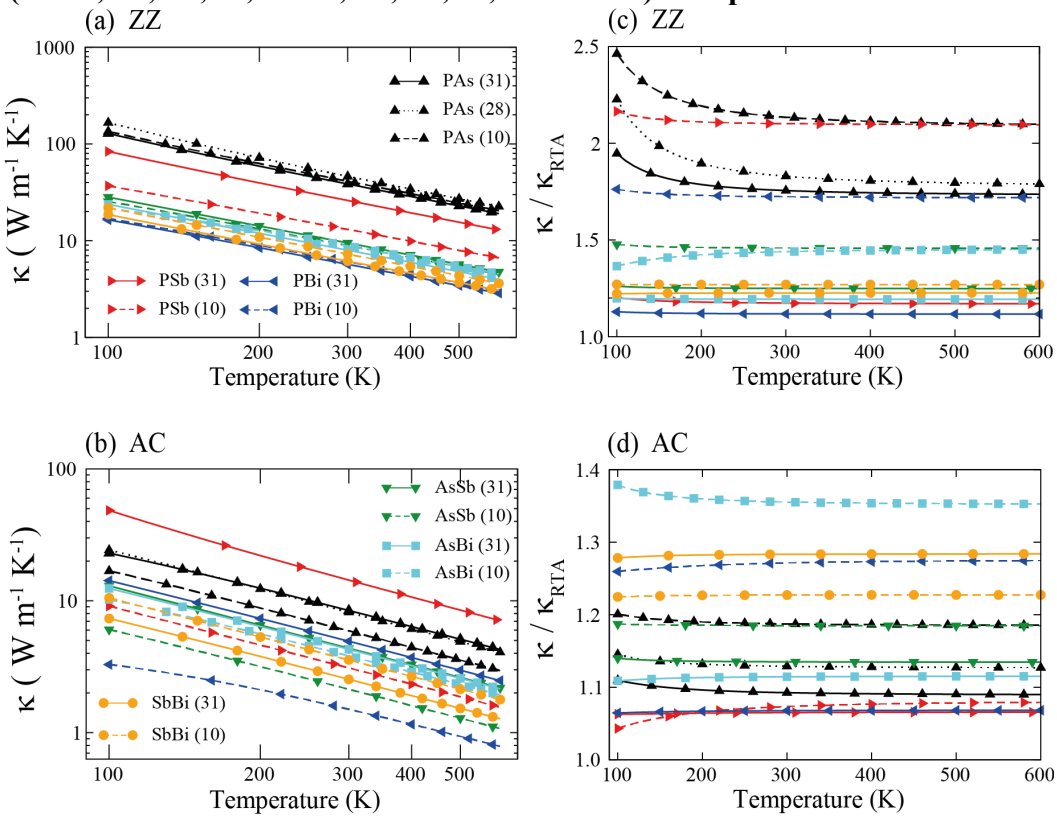

Figure 10: Thermal conductivity of 50% compound structures as a function of temperature along the (a) zigzag and (b) armchair direction calculated by the self-consistent solution of Peierls-BTE and ratio of the self consistent (κ) and zeroth order (corresponding to the κ_{RTA}) solutions are also depicted for (c) zigzag and (d) armchair directions.

c. X_1Y_3, (X = P, As, Sb Y = P, As, Sb and X ≠ Y) Compound Structures

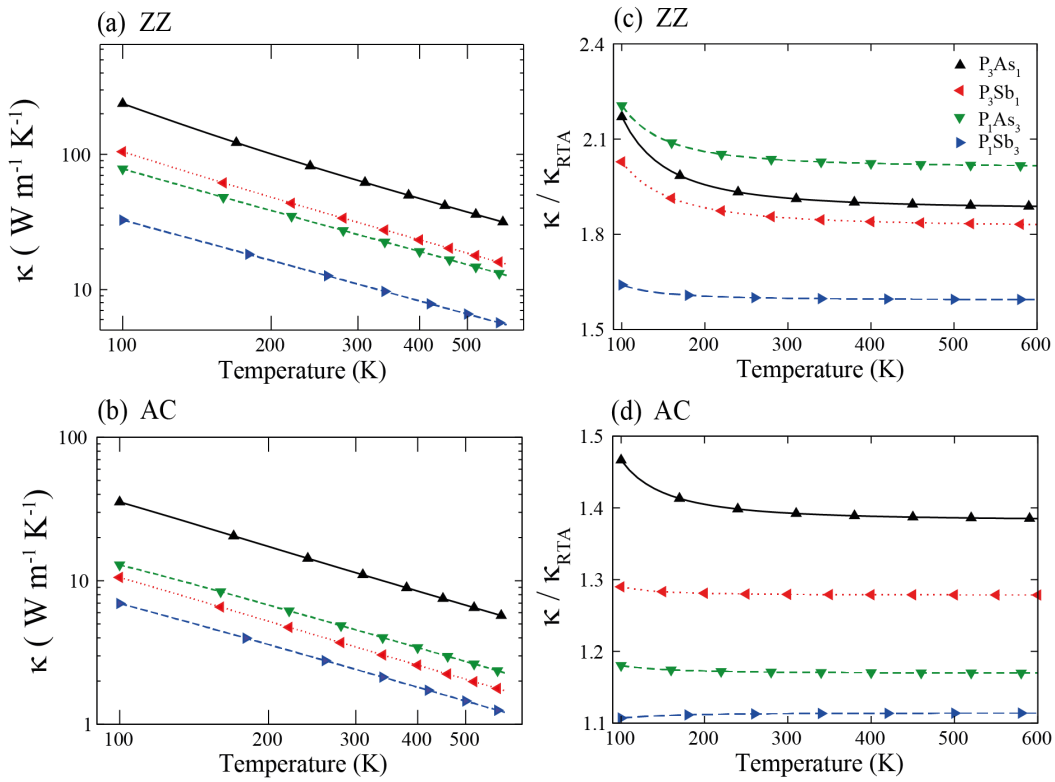

Figure 11: Thermal conductivity of 25% compound structures as a function of temperature along the (a) zigzag and (b) armchair direction calculated by the self-consistent solution of Peierls-BTE and ratio of the self consistent (κ) and zeroth order (corresponding to the κ_{RTA}) solutions are also depicted for (c) zigzag and (d) armchair directions.

10. Thermal Conductivity of Each Band

Here, each band correspond to the phonon modes, imply sorted based on the ascending order of the frequency.

a. Pristine Structure

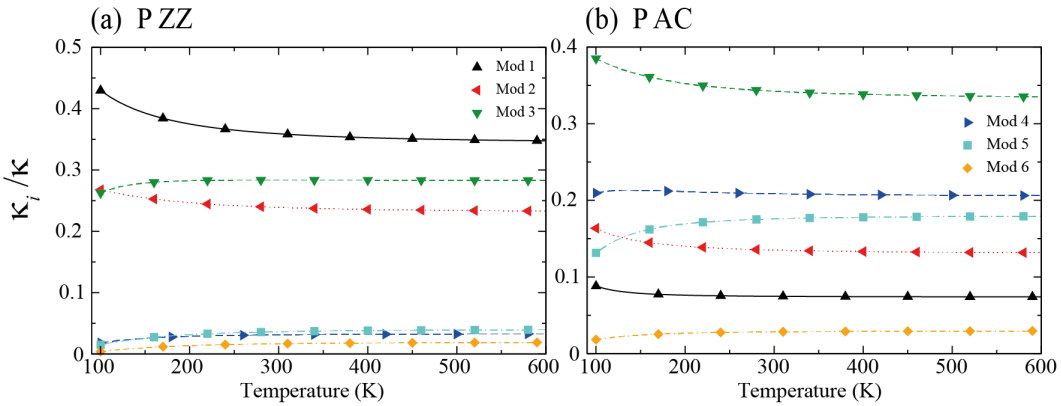

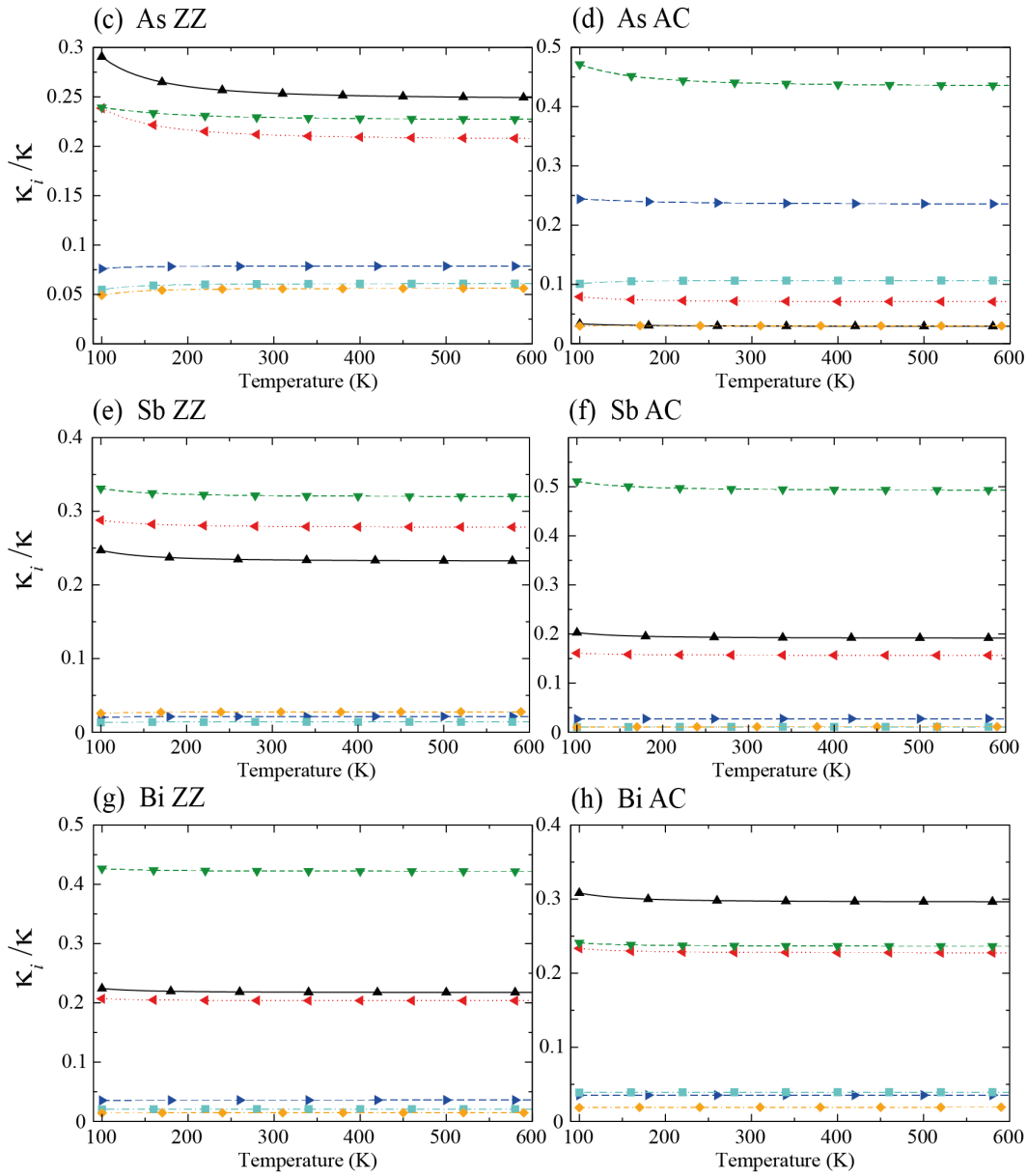

Figure 12: Normalized contribution of acoustic and low frequency optical phonon branches to the thermal conductivity as a function of temperature along the zigzag and armchair directions of pristine structures.

b. X_2Y_2, (X = P, As, Sb, Bi, Y = P, As, Sb, Bi, and X ≠ Y) Compound Structures

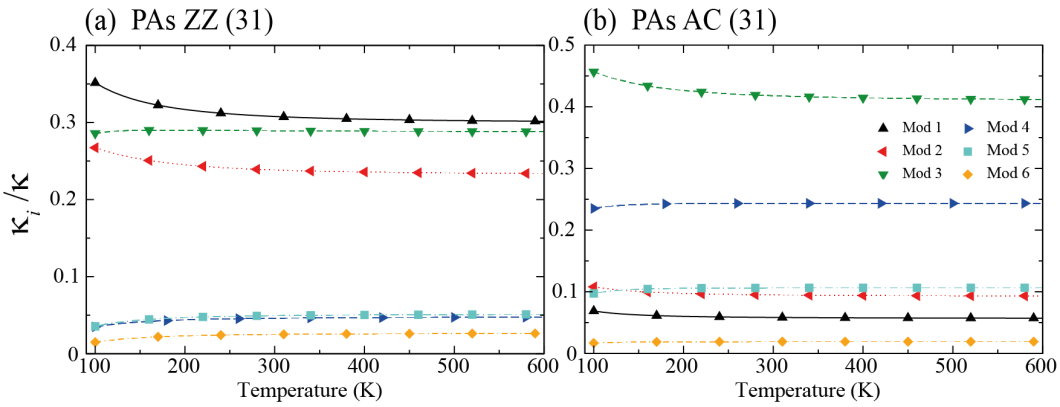

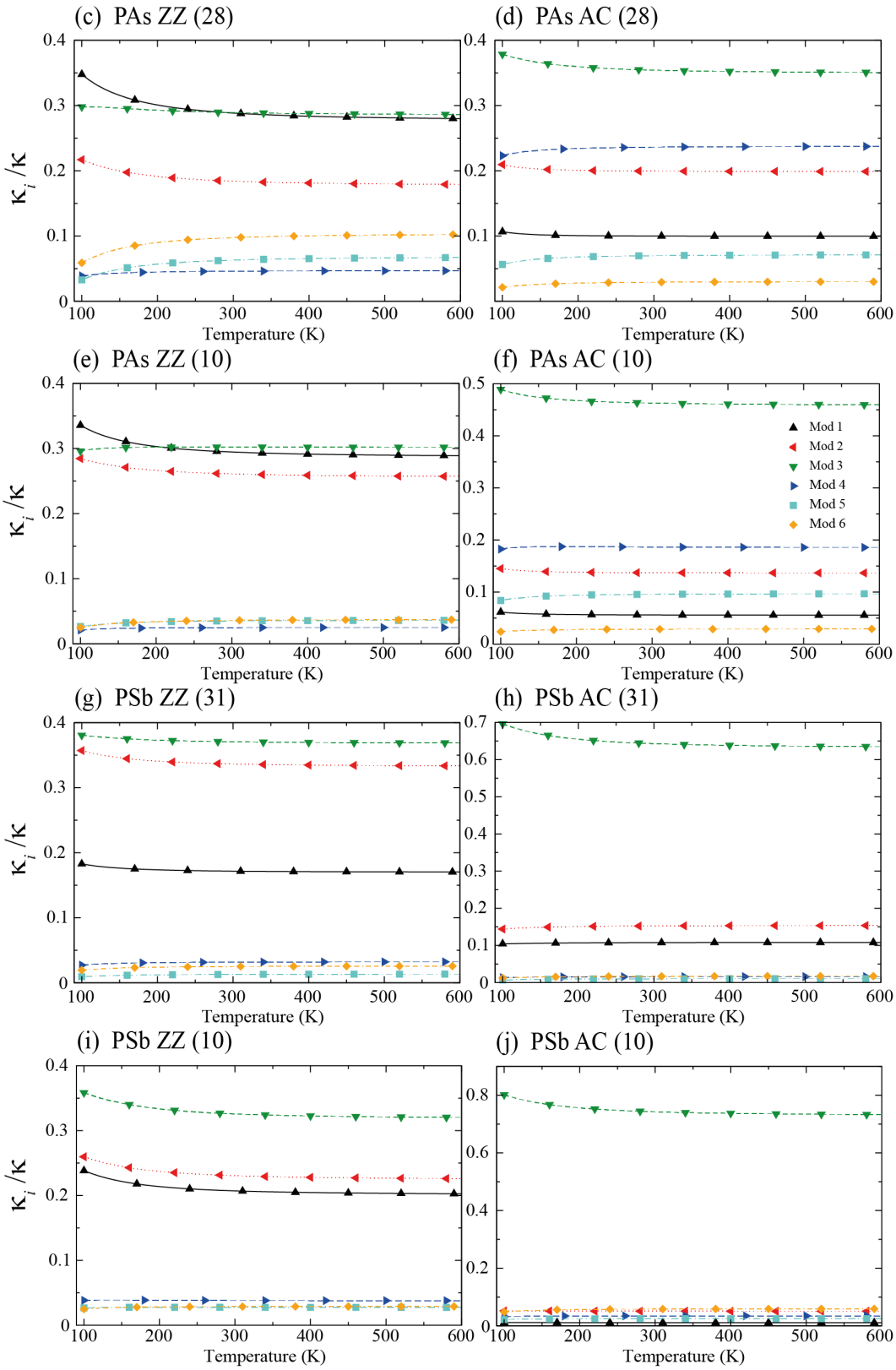
(c) PAs ZZ (28)
(d) PAs AC (28)
(e) PAs ZZ (10)
(f) PAs AC (10)
(g) PSb ZZ (31)
(h) PSb AC (31)
(i) PSb ZZ (10)
(j) PSb AC (10)
κi /κ
Temperature (K)
Mod 1
Mod 2
Mod 3
Mod 4
Mod 5
Mod 6

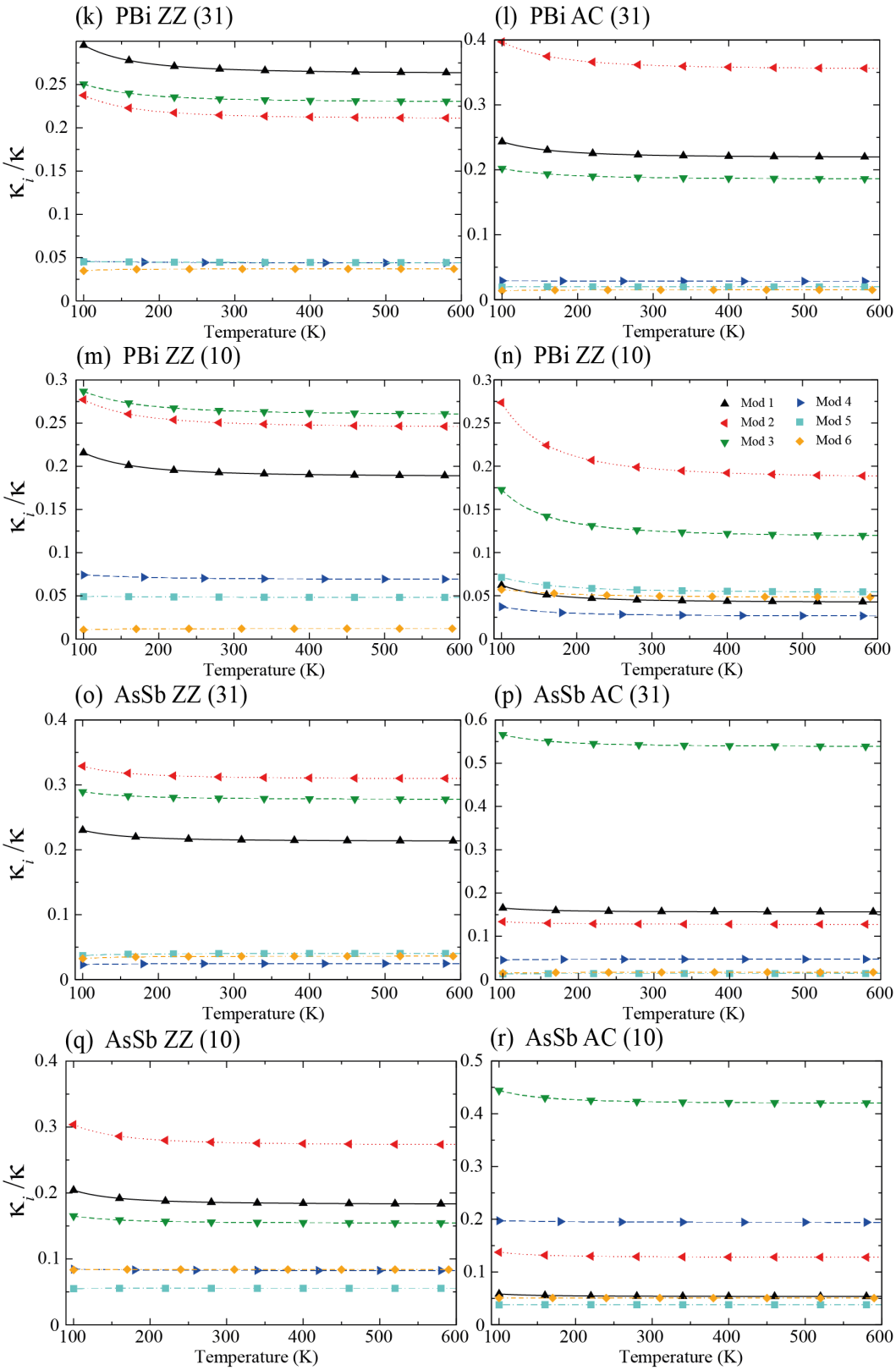
(k) PBi ZZ (31)
(l) PBi AC (31)
(m) PBi ZZ (10)
(n) PBi ZZ (10)
(o) AsSb ZZ (31)
(p) AsSb AC (31)
(q) AsSb ZZ (10)
(r) AsSb AC (10)
κ_i /κ
Temperature (K)
Mod 1
Mod 2
Mod 3
Mod 4
Mod 5
Mod 6

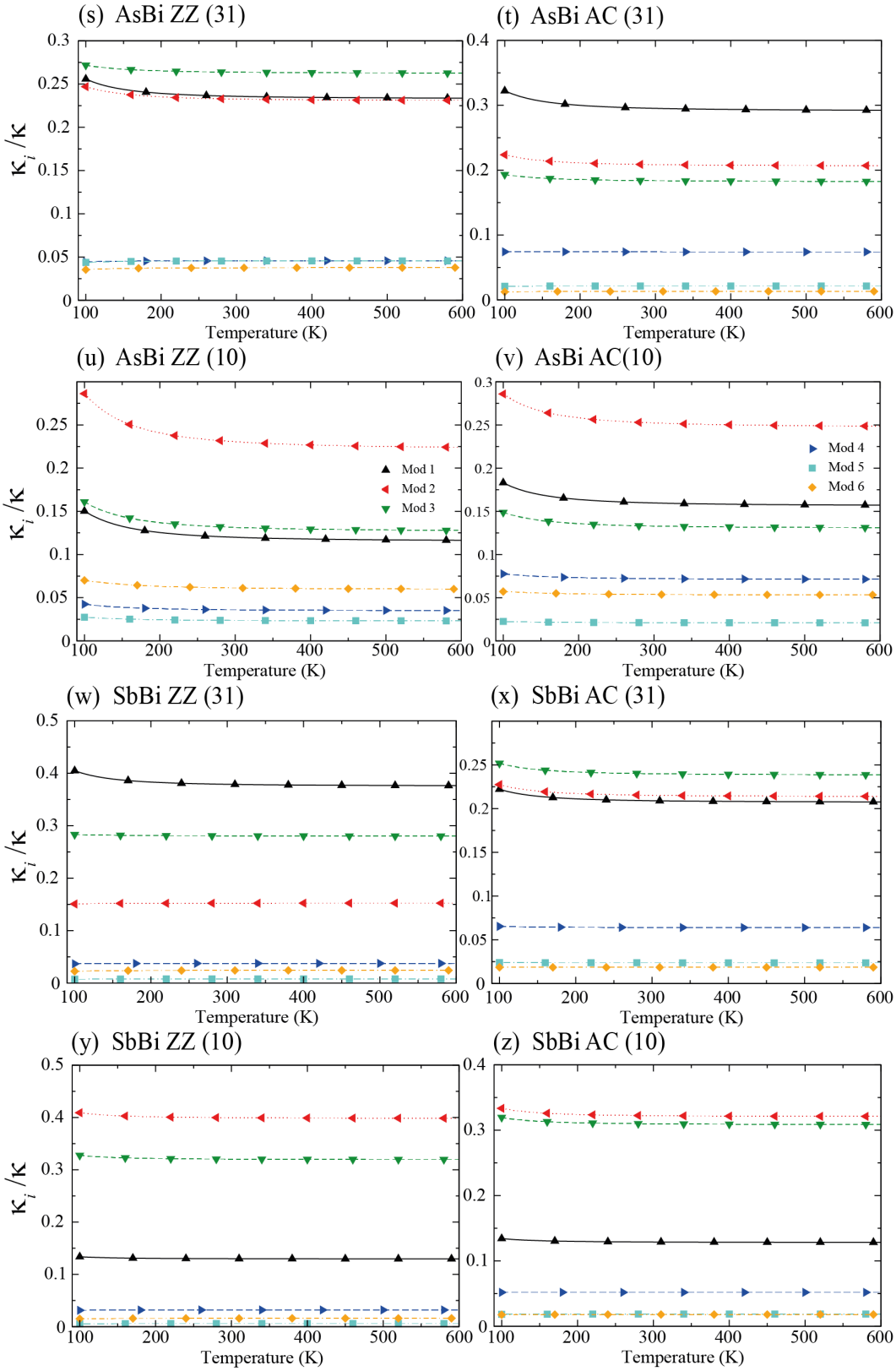

Figure 13: Normalized contribution of acoustic and low frequency optical phonon branches to the thermal conductivity as a function of temperature along the zigzag and armchair directions of 50% compound structures.

c. X_1Y_3, (X = P, As, Sb Y = P, As, Sb and X ≠ Y) Compound Structures

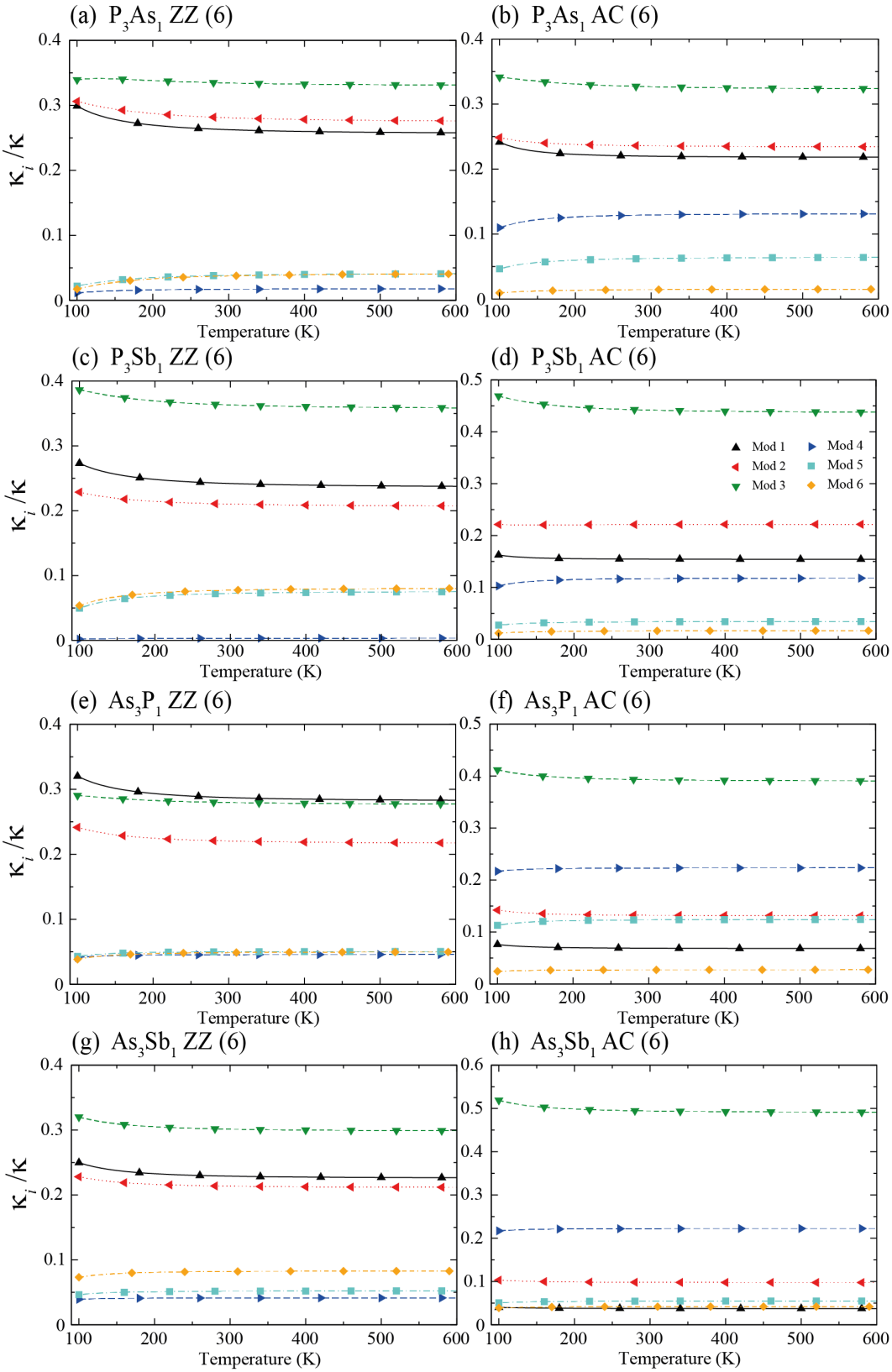

Figure 14: Normalized contribution of acoustic and low frequency optical phonon branches to the thermal conductivity as a function of temperature along the zigzag and armchair directions of 25% compound structures.

10. Relaxations Times

Here, each band correspond to the phonon modes, imply sorted based on the ascending order of the frequency.

a. Pristine Structures

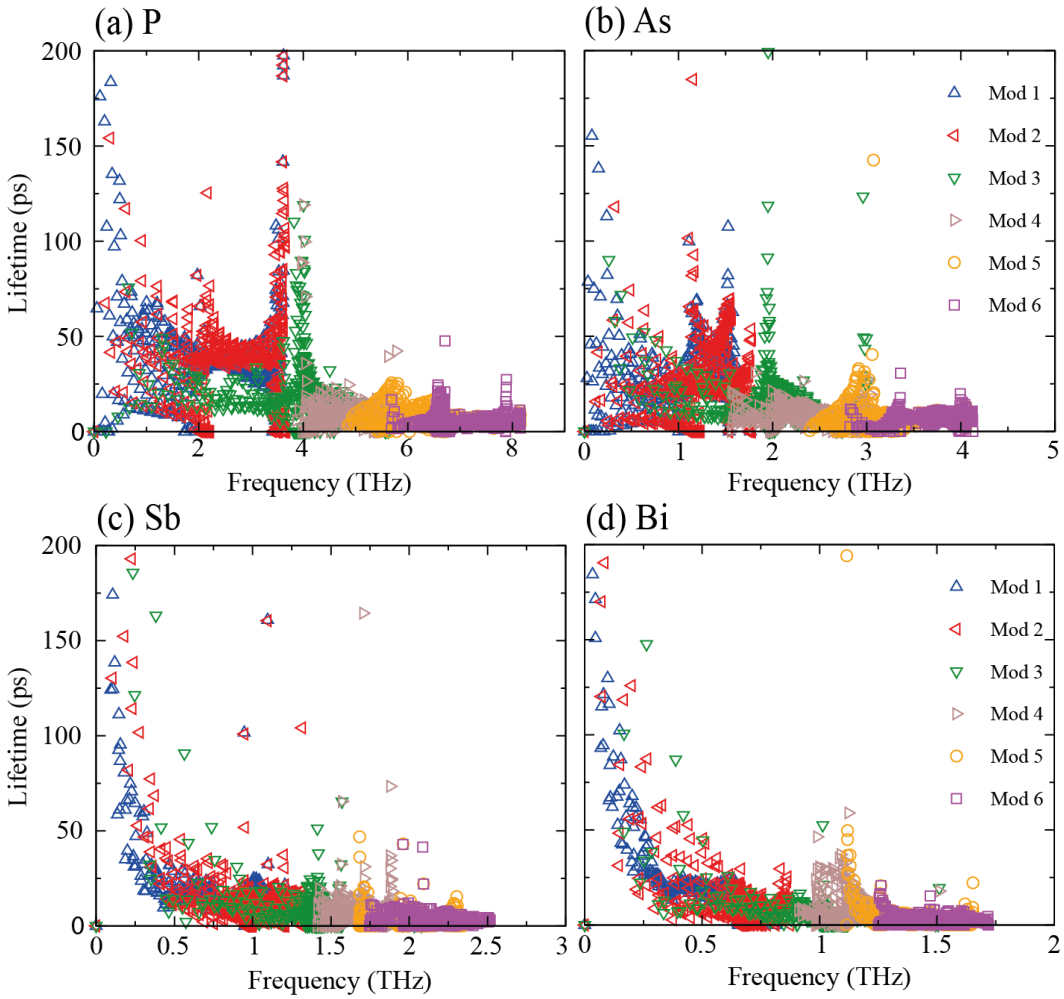

Figure 18: Relaxation time of phonon modes of pristine structures as a function of frequency for acoustic and low frequency optical phonons of pristine structures at T=300K

b. X_2Y_2, (X = P, As, Sb, Bi, Y = P, As, Sb, Bi, and X ≠ Y) Compound Structures

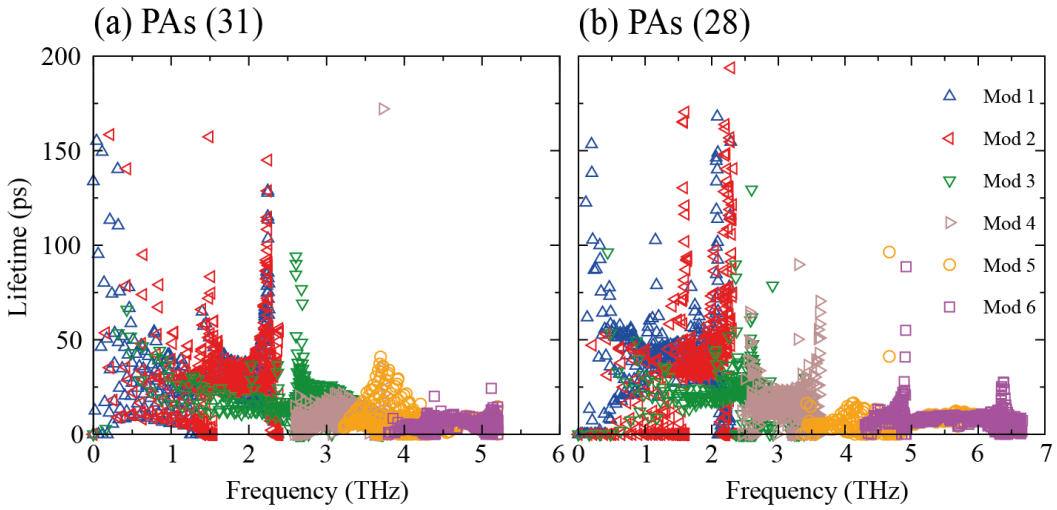

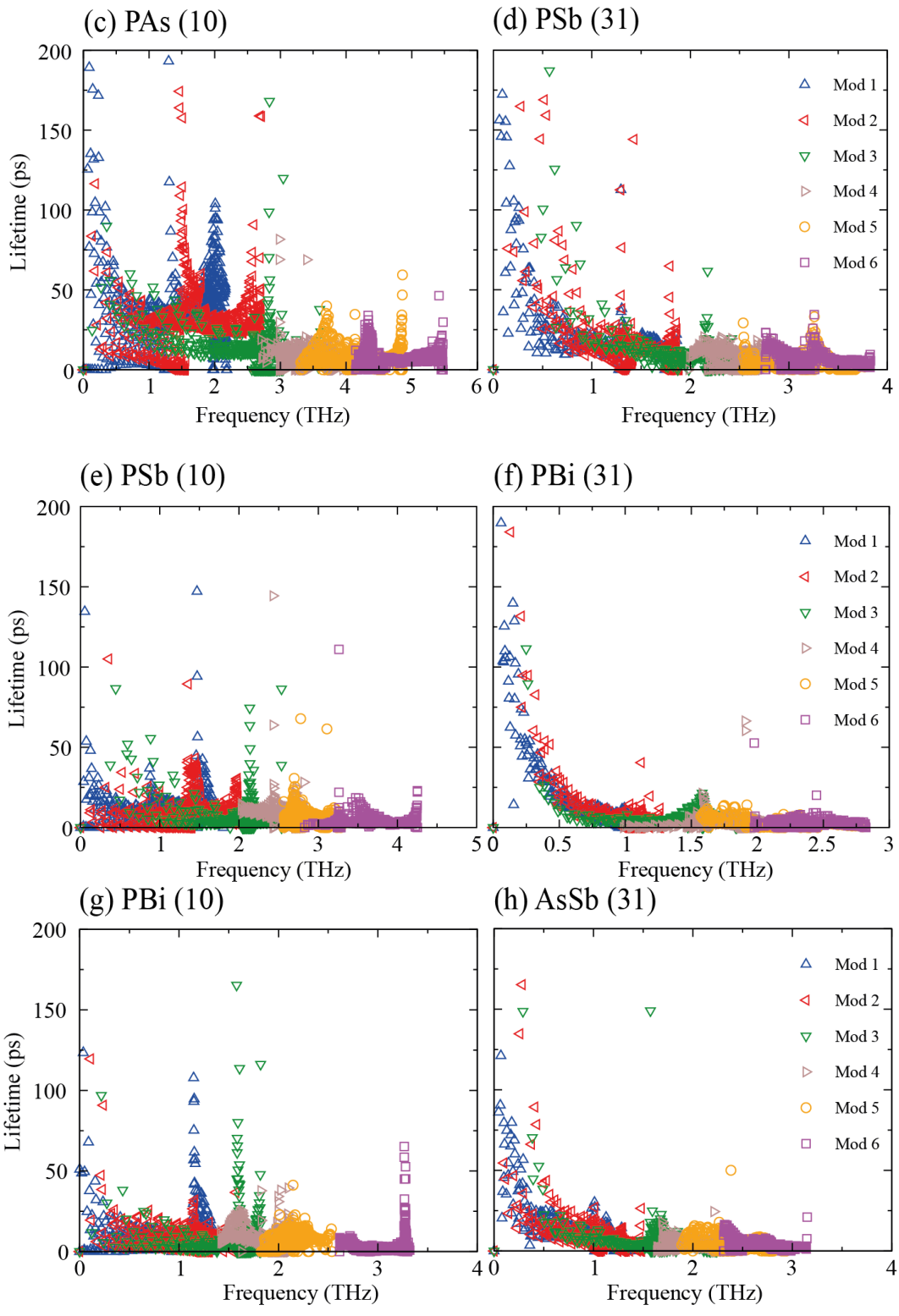
(c) PAs (10)
(d) PSb (31)
(e) PSb (10)
(f) PBi (31)
(g) PBi (10)
(h) AsSb (31)
Lifetime (ps)
Frequency (THz)
Mod 1
Mod 2
Mod 3
Mod 4
Mod 5
Mod 6

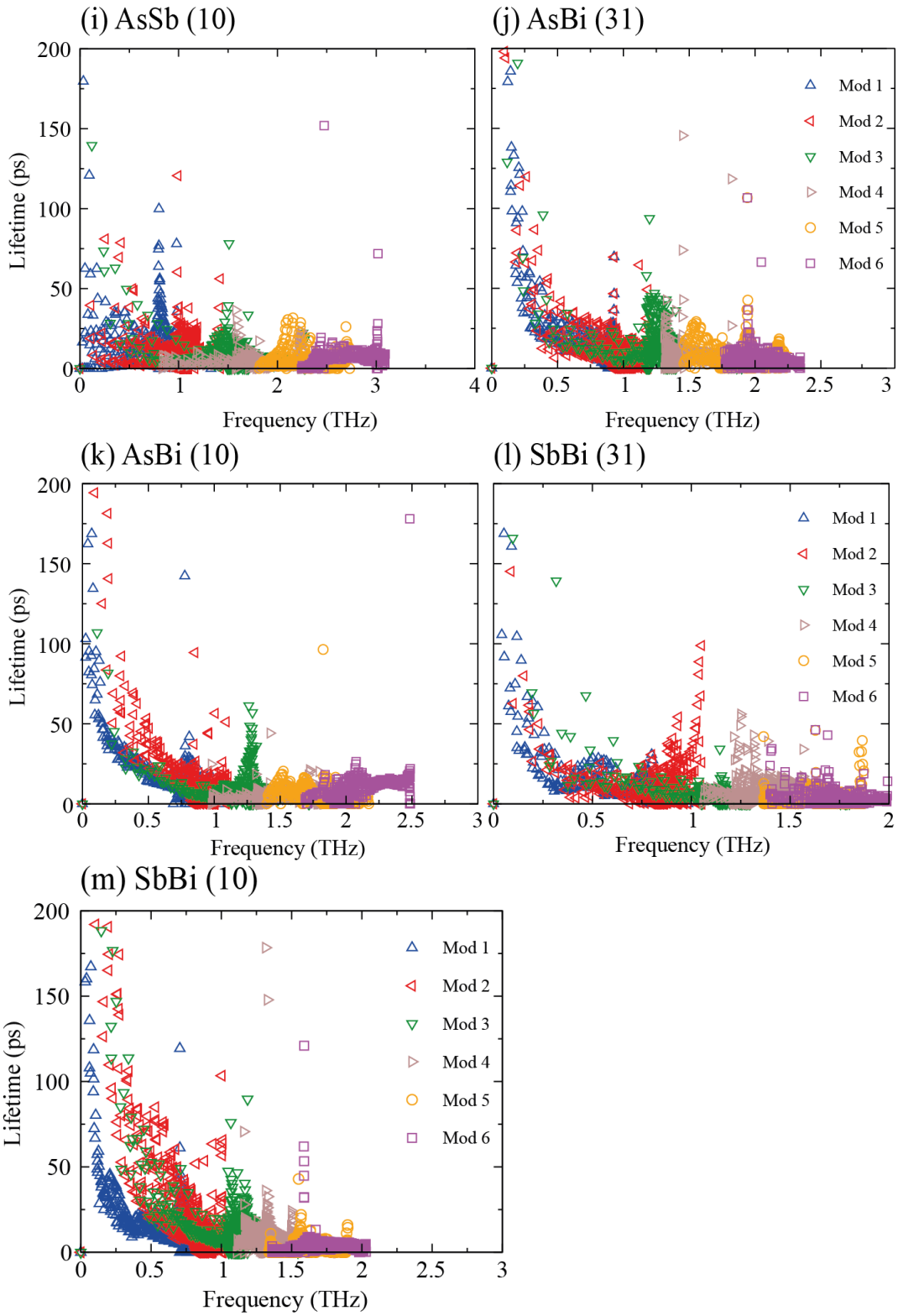

Figure 19: Relaxation time of phonon modes of 50% compound structures as a function of frequency for acoustic and low frequency optical phonons of pristine structures at T=300K

c. X_1Y_3, (X = P, As, Sb Y = P, As, Sb and X ≠ Y) Compound Structures

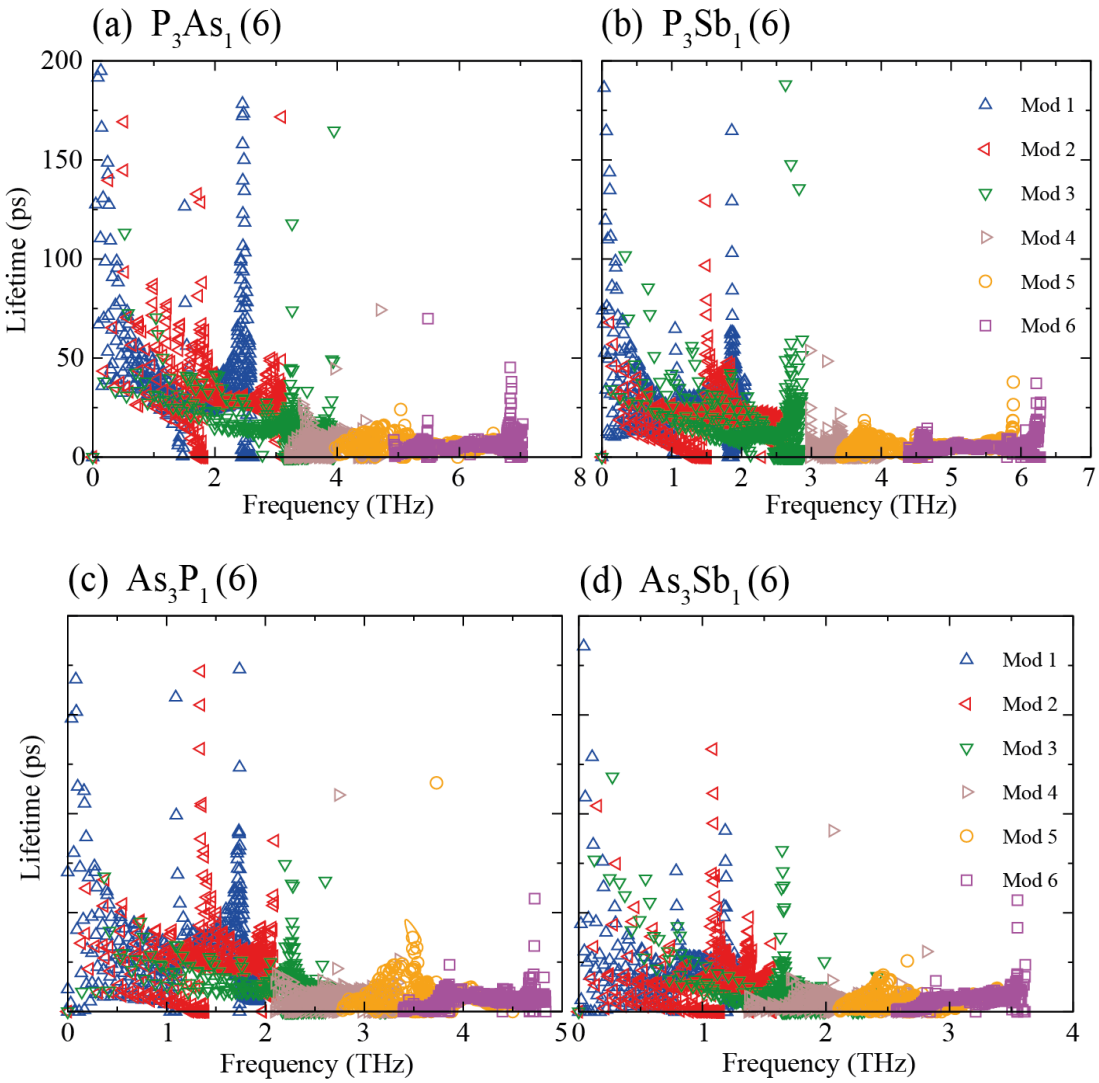

Figure 20: Relaxation time of phonon modes of 25% compound structures as a function of frequency for acoustic and low frequency optical phonons of pristine structures at T=300K

11. Convergence of Thermal Conductivity with q-grid

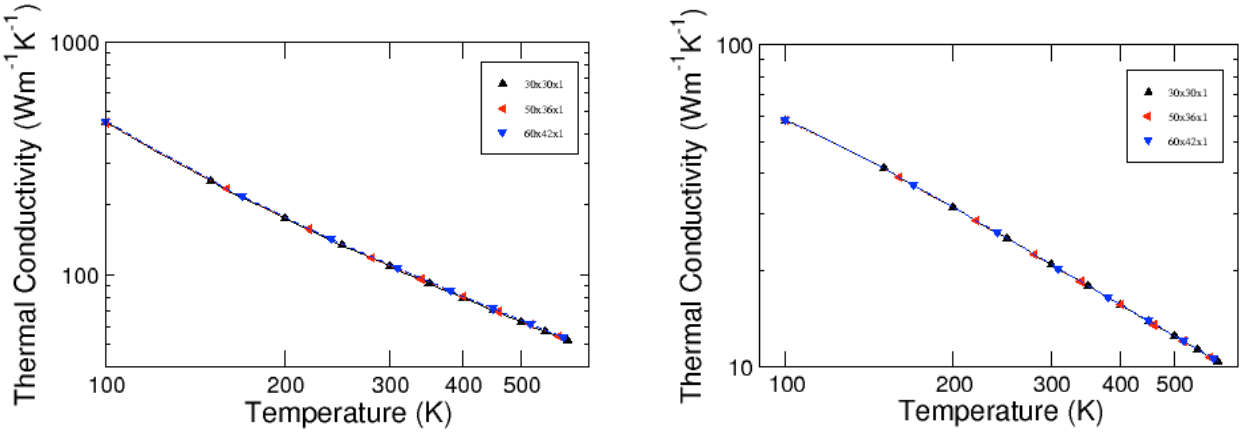

Figure 21: Convergence of calculated thermal conductivity of Phosphorene with q-grid.